

# High-order clustering of WiggleZ galaxies

F A Marín and The WiggleZ Team<sup>1</sup>

Centre for Astrophysics and Supercomputing, Swinburne University of Technology, P.O. Box 218, Hawthorn, VIC 3122, Australia

E-mail: fmarin@astro.swin.edu.au

**Abstract.** High-order statistics are a useful and complementary tool for measuring the clustering of galaxies, containing information on the non-Gaussian evolution and morphology of the large structures in the Universe. In this work, we have presented results of the 3-point correlation function in the WiggleZ spectroscopic galaxy survey, at three different epochs. Using N-body simulations to predict the clustering of matter, we have constrained the linear and non-linear bias parameters of WiggleZ galaxies with respect to total matter, and marginalized over them to obtain constraints on  $\sigma_8(z)$ , the variance of perturbations, and its evolution with redshift. These measurements are consistent with the predictions of the  $\Lambda$ CDM concordance cosmology and test this model in a new way.

## 1. Introduction

In the current structure formation paradigm [1], galaxies are formed inside dark matter halos, which evolved from small perturbations in the early universe, allowing us to connect the galaxy field with the cosmological models of structure formation. This connection, however, is not a perfect one, since galaxy observables such as luminosity, colour, etc. are also shaped by baryonic physics, leading to systematics and degeneracies when using clustering statistics of galaxies to extract information on cosmological parameters, and therefore, it is necessary to resort to other observables or objects to break these degeneracies. One way to use the *same data sample* to separate the galaxy formation imprints in the large-scale clustering from the cosmological background are the higher-order correlations functions [2].

In this work, we have presented results of the measurement of the 3-point correlation function (3PCF) for a sample of 187,000 spectroscopy-selected galaxies from the WiggleZ galaxy survey [3], with galaxies in the range  $0.1 < z < 1.0$  at a median redshift of  $z \sim 0.6$ . Using N-body simulations to study dark matter statistics, we have estimated the WiggleZ galaxy bias to put constraints on the parameter  $\sigma_8$ , the rms over-density of spheres at a radius  $8 h^{-1}$  Mpc, which provides a normalization of the primordial power spectrum. Also, we have splitted our galaxy sample in redshift slices, which allow us to measure  $\sigma_8$  as a function of redshift, and in this way get constraints on the structure growth history.

## 2. Data and simulations

The WiggleZ Dark Energy Survey has obtained spectroscopic redshifts of galaxies over a cosmic volume of approximately  $1 \text{ Gpc}^3$  in the range  $0 < z < 1$ , measured on 3.9 m Anglo-Australian

<sup>1</sup> <http://wigglez.swin.edu.au/site/team.html>



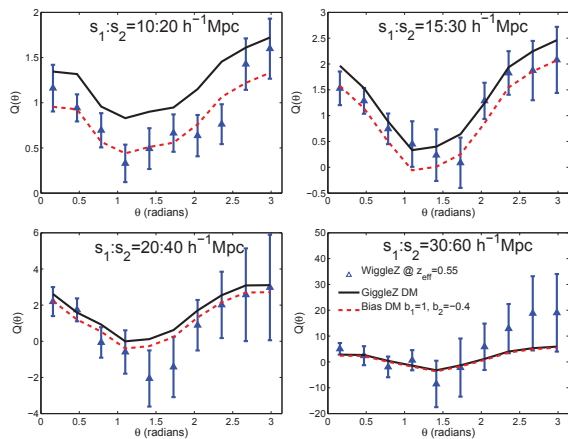


**Figure 1.** The redshift-space reduced 3PCF,  $Q(s_1, s_2, \theta)$  of WigglerZ galaxies in the  $z_{\text{eff}} = 0.55$  slice (blue triangles), and of total matter from the GigglerZ simulation (black solid line), and the best bias model (red dashed line) for different sets of scales  $s_1$ .

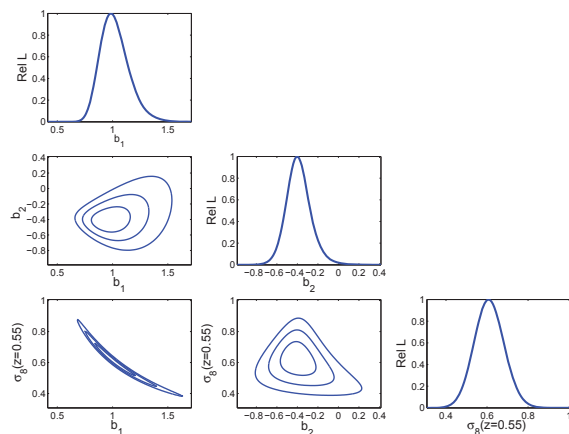


**Figure 2.** Constraints in the bias parameters and  $\sigma_8$  from the redshift-space 2PCF and 3PCF for WigglerZ galaxies in the  $z_{\text{eff}} = 0.55$  slice. The contours represent  $1\sigma$ ,  $2\sigma$  and  $3\sigma$  joint confidence regions for a two-parameter fit.

Telescope. Target galaxies in seven different regions were chosen using UV photometric data from the *GALEX* survey [4], matched with optical photometry from the Sloan Digital Sky Survey [5], and the Red Sequence Cluster Survey 2 [6], applying magnitude and colour cuts to select star-forming galaxies with bright emission lines in a redshift distribution centred around  $z \sim 0.6$ . To study the evolution of clustering with redshift, we have used three overlapping slices of redshifts [0.1, 0.5], [0.4, 0.8], and [0.6, 1.0] with effective (correlation-function averaged) redshifts of  $z_{\text{eff}} = [0.35, 0.55, 0.68]$  respectively.

The dark matter correlation functions have been measured on the GigglerZ simulations [7]. In a  $1 (h^{-1}\text{Gpc})^3$  periodic cube,  $2160^3$  dark matter particles with individual masses of  $m_p = 7.5 \times 10^9 h^{-1}M_\odot$  are evolved on a WMAP-5 cosmology [8]. In order to compare the correlation functions of WigglerZ galaxies and dark matter, we have measured them in snapshots of the simulation at the effective redshift of the WigglerZ sub-samples.

### 3. The WigglerZ 3-point correlation function

The galaxy  $n$ -point correlation functions are the average of galaxy over-density  $\delta_g$  measured at  $n$  different points [2]. Whereas, the 2-point correlation function  $\xi(r)$  (2PCF) depends only on the scale of clustering  $r$ , but the 3-point correlation function  $\zeta(r_1, r_2, r_3)$  (3PCF), is sensitive as well to the shapes of spatial structures [9]. We have calculated the 2PCF and 3PCF using estimators, which count pairs and triplets in the galaxy data and random catalogues, optimally correcting for edge effects and incompleteness of the survey [10, 11]. The random catalogues were built taking into account the radial selection function and angular completeness [12], and the covariance matrix is calculated from jack-knife re-sampling of the different regions. To count the pairs and triplets, we use the *ntropy-npoint*, which is an exact  $n$ -point calculator, which uses a kd-tree framework with enhanced routine performance [13, 14].

We have shown our measurements in terms of the redshift-space reduced 3PCF,  $Q(s_1, s_2, \theta) = \zeta(s_1, s_2, s_3) / [\xi(s_1)\xi(s_2) + \text{perm}]$ , where  $\theta$  is the angle between the first two sides  $s_1$  and  $s_2$ , which determines  $s_3$ . Figure 1 shows  $Q(s_1, s_2, \theta)$  of the WigglerZ galaxies (from optimally combining the seven independent regions) in the intermediate redshift slice,  $z_{\text{eff}} = 0.55$  for a range of scales,

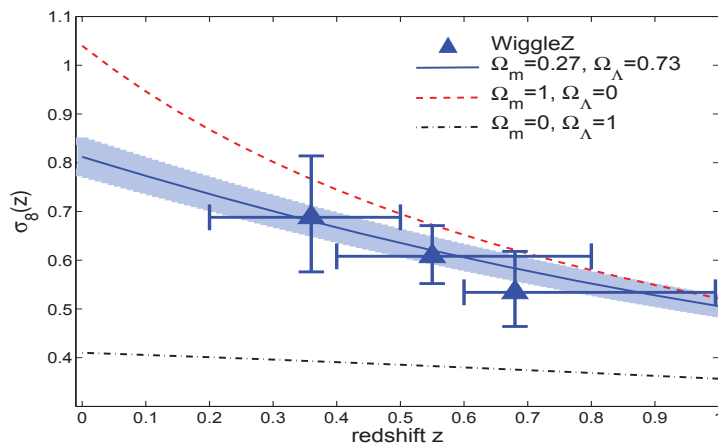


**Figure 3.** Evolution of  $\sigma_8(z)$ . Blue symbols correspond to the estimates of  $\sigma_8(z_{\text{eff}})$  from the 2PCF and 3PCF of WiggleZ galaxies at different redshifts, marginalizing over the linear and non-linear bias parameters. Blue solid line corresponds to the evolution of  $\sigma_8(z)$  in a flat  $\Lambda$ CDM universe, with  $\Omega_m = 0.27$  and  $\sigma_8(z = 0) = 0.812$ ; blue shaded region corresponds to combined WMAP-5 errors. Red dashed line corresponds to the evolution of  $\sigma_8(z)$  in a flat  $\Omega_m = 1$  CDM universe. Black dash-dotted line shows the evolution of a flat  $\Omega_\Lambda = 1$  universe. All models are normalized at the epoch of recombination.

where the  $s_2 = 2s_1$  as a function of  $\theta$ . It can be seen that we recover the shape dependence of the 3PCF, observed on smaller redshifts [14, 15], where there is a bigger 3PCF amplitude at very small or large  $\theta$ , i.e., the collapsed and elongated configurations. This ‘V-shape’ is more prominent on large scales; it is a consequence of the morphology of galaxy structures going from spherically-shaped clusters and groups on small  $\sim 1 h^{-1}\text{Mpc}$  scales, to filaments on the largest scales. The dark matter reduced 3PCF follows the same characteristics of the WiggleZ 3PCF, and moreover, the difference in amplitude in  $Q(\theta)$  is small, contrary to what is found in other types of galaxies (e.g., LRGs [15]), which is indicative of differences of the dark matter halos that host different types of galaxies [16].

#### 4. Constraints on galaxy bias and $\sigma_8(z)$

Since different types of galaxies form inside different dark matter halos, they are an imperfect tracer of dark matter [16], and their  $n$ -point correlations will differ as well. To model these differences, we have adopted a deterministic and local bias formalism to relate galaxy overdensity  $\delta_g$  with the underlying dark matter density  $\delta_{dm}$  [17, 18], where  $\delta_{gal} = b_1\delta_{dm} + (b_2/2)\delta_{dm}^2$ . As a consequence of adopting this model, the 2PCF and the 3PCF of dark matter and galaxies are related by these bias parameters  $b_1, b_2$ . In addition to this, the total amplitude of the correlation functions depends on the amplitude of the initial perturbations, in the form of the parameter  $\sigma_8$ . At leading order, for the 2PCF,  $\xi \propto \sigma_8^2$  and for the 3PCF,  $\zeta \propto \sigma_8^4$  [19], we have then,

$$\xi_{gal} = b_1^2 \left( \frac{\sigma_8}{\sigma_8^{fid}} \right)^2 \xi_{dm, \sigma_8^{fid}}, \quad \text{and} \quad Q_{gal} = \frac{1}{b_1} \left( Q_{dm} + \frac{b_2}{b_1} \right), \quad (1)$$

where  $\sigma_8^{fid}(z = 0) = 0.812$ , the value used in our GigggleZ simulations. Though these relations are valid only on large scales (where perturbations are mildly non-linear) and in real space, with

the level of the statistical errors of our measurements, it is adequate to use them in redshift space [20, 21, 15]. Therefore, the reduced 3PCF  $Q$  breaks the degeneracy between the linear bias and  $\sigma_8$  in the 2PCF.

Comparing both the 2PCF and 3PCF for configurations with  $s_1 > 10 h^{-1}\text{Mpc}$ , from WiggleZ galaxies and the biased dark matter model from the GigggleZ simulation, we have used a  $\chi^2$ -minimization procedure to estimate the bias parameters  $b_1$ ,  $b_2$  and  $\sigma_8$ . In Figure 2, we have shown the constraints in the  $z_{\text{eff}} = 0.55$  redshift slice. Even though the confidence intervals are bigger than other measurements at lower redshifts [21, 22, 15], the value of the linear bias  $b_1 \sim 1$  indicates that WiggleZ galaxies are hosted by low-to-intermediate mass dark matter halos. In addition, we have detected a non-zero value for the non-linear bias  $b_2 \sim -0.4$ . For  $\sigma_8$ , the  $1\sigma$  values are inside of what is expected at that redshift from the WMAP-5 cosmology (where  $\sigma_8^{\text{fid}} = 0.62$  at  $z=0.55$ ). It is important to note that these estimates are independent of any other observable than the galaxy clustering itself.

We have repeated the measurement and analysis of the correlation functions for the other two redshift slices, in order to get constraints on  $\sigma_8$  as a function of redshift. The evolution of this parameter gives us an indication on how the linear growth factor  $D(z)$  evolves with redshift, since  $\sigma_8(z) = [D(z)/D(0)]\sigma_8(0)$ . In Figure 3, we have plotted  $\sigma_8$  as a function of redshift for our measured values in the WiggleZ survey, and though the measurements of the different redshift slices are correlated, given that they overlap, we have found a good agreement with the measurements of WMAP-5 in a concordance cosmology. In the near future, with improved measurement techniques and with the arrival of bigger surveys, we will be able to use this method to get constraints not only on  $\sigma_8$  in the context of the  $\Lambda\text{CDM}$  model, but also to discriminate it against modified gravity models [23].

## References

- [1] Press W H and Schechter P 1974 *Ap. J.* **187** 425
- [2] Peebles P J E 1980 *The Large-Scale Structure of the Universe* (Princeton University Press)
- [3] Drinkwater M J *et al* 2010 *MNRAS* **401** 1429 [arXiv:0911.4246]
- [4] Martin D C *et al* 2005 *Ap. J.* **619** L1 [arXiv:astro-ph/0411302]
- [5] Adelman-McCarthy J K *et al* 2006 *Ap. J. Supp.* **162** 38
- [6] Gilbank D G, Gladders M D, Yee H K C and Hsieh B C 2011 *Astron. J.* **141** 94 [arXiv:1012.3470]
- [7] Poole G *et al* 2012 *In preparation*
- [8] Komatsu E *et al* 2009 *Ap. J. Supp.* **180** 330 [arXiv:0803.0547]
- [9] Peebles P J E and Groth E J 1975 *Ap. J.* **196** 1
- [10] Landy S D and Szalay A S 1993 *Ap. J.* **412** 64
- [11] Szapudi S and Szalay A S 1998 *Ap. J. Lett.* **494** L41
- [12] Blake C *et al* 2010 *MNRAS* **406** 803 [arXiv:1003.5721]
- [13] Gardner J P, Connolly A and McBride C 2007 *Astronomical Data Analysis Software and Systems XVI (ASP Conf. Ser.* **376** ed. R A Shaw, F Hill, and D J Bell 69
- [14] McBride C K, Connolly A J, Gardner J P, Scranton R, Newman J A, Scoccimarro R, Zehavi I and Schneider D P 2011 *Ap. J.* **726** 13 [arXiv:1007.2414]
- [15] Marín F 2011 *Ap. J.* **737** 97 [arXiv:1011.4530]
- [16] Berlind A A and Weinberg D H 2002 *Ap. J.* **575** 587
- [17] Fry J N and Gaztanaga E 1993 *Ap. J.* **413** 447
- [18] Frieman J A and Gaztanaga E 1994 *Ap. J.* **425** 392
- [19] Pan J and Szapudi I 2005 *MNRAS* **362** 1363
- [20] Scoccimarro R, Couchman H M P and Frieman J A 1999 *Ap. J.* **517** 531
- [21] Gaztañaga E, Norberg P, Baugh C M and Croton D J 2005 *MNRAS* **364** 620
- [22] McBride C K, Connolly A J, Gardner J P, Scranton R, Scoccimarro R, Berlind A A, Marín F and Schneider D P 2011 *Ap. J.* **739** 85 [arXiv:1012.3462]
- [23] Linder E V and Cahn R N 2007 *Astroparticle Phys.* **28** 481 [arXiv:astro-ph/0701317]